Bimodal SLD Ice Accretion on a NACA 0012 Airfoil Model

Mark G. Potapczuk[1]
NASA John H. Glenn Research Center, Cleveland, Ohio, 44135 USA

Jen-Ching Tsao[2]
Ohio Aerospace Institute, Cleveland, Ohio, 44135 USA

Laura E. King-Steen[3]
HX5 Sierra, Cleveland, Ohio, 44135 USA

An initial ice shape database has been created to document ice accretions on a 21-inch chord NACA 0012 airfoil model resulting from an exposure to a Supercooled Large Droplet (SLD) icing cloud with a bimodal droplet distribution. The ice shapes created were documented with photographs, laser scanned surface measurements over a section of the model span, and measurement of the ice mass over the same section of each accretion. The icing conditions used in the test matrix were based upon previously measured ice shapes on the same model to connect the current database to previously measured information. Ice shapes resulting from the bimodal distribution as well as from equivalent standard droplet distributions were obtained and compared. Results indicate that the ice shapes resulting from the bimodal droplet distributions had higher mass and volume values than their standard distribution equivalents as well as having icing limits that extended further back on the chord of the model.

I. Introduction

Ice accretion on aircraft surfaces as a result of exposure to supercooled large droplets (SLD) is an area of continued research interest to the aerospace community. Methods for simulation of SLD conditions in ground based experimental facilities and within computational tools are currently under development at industrial, academic and governmental institutions around the world. It is clear that most experimental facilities can reproduce aspects of an SLD icing encounter and equally clear that no one facility can reproduce all aspects of an SLD icing cloud. Likewise, computational tools have been developed that can incorporate elements of SLD icing physics however a lack of information concerning the complete range of SLD conditions limits the validation of such tools.

At the NASA Glenn Research Center, work has been underway to extend the capabilities of the Icing Research Tunnel (IRT) to include a broader range of SLD conditions.[1] In addition to a broader range of conditions represented by droplet distribution curves having a classic bell shape curve, the simulation of a bimodal drop size distribution representative of the freezing drizzle (FZDZ), MVD < 40 μm distributions contained within Federal Aviation Administration (FAA) regulations[2] for SLD has been developed.[3] This drop-size distribution has been created in the IRT and measured to match the FAA Appendix O normalized cumulative distribution within 10% of the total volume for all drop sizes. Furthermore, these bimodal cloud development tests showed experimentally that for two different cases simulated, the measured combined

[1] Research Aerospace Engineer, Icing Branch, 21000 Brookpark Road, MS 11-2.
[2] Principal Research Scientist, 21000 Brookpark Road, MS 11-2, Associate Fellow AIAA.
[3] Icing Cloud Calibration Engineer, Test Engineering Services, 21000 Brookpark Road, MS 6-2, AIAA Member

drop-size distributions from two nozzle spray conditions matched the mathematical sum of the two conditions sprayed individually.

The focus of this paper is to report on an examination of the ice shapes that are produced with this bimodal distribution and to compare such shapes to those formed with similar cloud conditions using standard single nozzle spray conditions. The resulting ice shapes are compared by evaluating cross sections of the shapes and ice shape volumes obtained from laser scan data as well as mass measurements made during the testing. This data will provide some insight into the characteristics that differentiate single spray conditions from bimodal spray conditions. This in turn should enable researchers to determine whether bimodal spray cloud recreation is necessary for accurate reproduction of SLD icing conditions.

II. Facility, Model and Experimental Methods

A. Facility

The NASA Icing Research Tunnel is a closed-loop, atmospheric tunnel, with a 1.83 m by 2.74 m by 6.10 m (6 ft by 9 ft by 20 ft) test section. A tunnel schematic is shown in Fig. 1. The IRT's calibrated test section speed ranges between 50 and 350 knots. The test section temperature can be controlled between +10 °C total temperature to -35 °C static temperature.

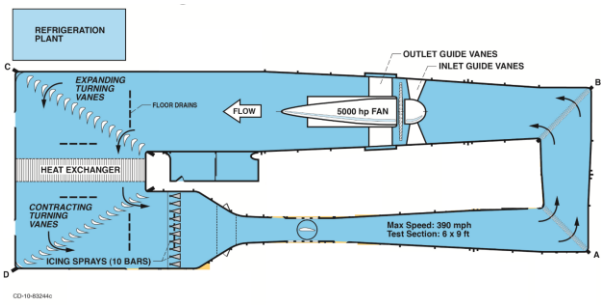

Figure 1. Schematic of the Icing Research Tunnel at NASA Glenn Research Center.

The spraybars that create the cloud are located just upstream of the contraction and consist of 10 bars, each of which has one air manifold and two water manifolds, which allows two nozzle sets to be run. There are two types of spray nozzles in the IRT spray bars: the Standard nozzles that have a higher water flow rate, and the Mod1 nozzles that have a lower water flow rate. Both nozzle types use internal mixing of air and water to create the cloud. The primary difference is in the diameter of the water hypodermic tubing used in the nozzles. There are currently 165 Standard nozzles and 88 Mod1 nozzles in the spray bars. The two nozzle sets may be sprayed individually, or if they are set at the same air pressure, they may be sprayed simultaneously, with different water pressures. Nozzle air pressure (p_{air}) and delta pressure (expressed as water pressure minus air pressure, or Dp) and nozzle type are varied to create the desired drop size and water content. All water supplied to the IRT spray bars has been filtered and de-ionized.

Drop sizes in the IRT are typically described in terms of median volumetric diameter (MVD), which is the drop diameter at which half the liquid water content volume is contained in smaller drops (and half in larger drops). Under "normal" operating conditions, when p_{air} is 10 psig or higher, the calibrated MVD range of the spray nozzles is between 14 and 50 μm for both nozzle sets. When the p_{air} is set below 10 psig, larger drops can be created, resulting in a calibrated MVD as high as 270 μm and maximum drop sizes as high as 1200 μm. This is typically only done with the Mod1 nozzles, since they have a lower flow rate, better matching to the requirements of large-drop certification criteria. The calibrated cloud liquid water content (LWC) range of the IRT is between 0.2 and 4.5 g/m^3. A full report on the cloud calibration of the IRT can be found in Ref. 1.

King-Steen and Ide have developed an approach to reproduce droplet distributions that are quite close to the freezing drizzle, MVD < 40 μm condition from Appendix O. Their approach is based upon simultaneous spray from both the Mod1 and Standard nozzles. As noted earlier, all the nozzles in the IRT

are connected to the same air manifold, however, the Mod1 and Standard nozzles each have their own water manifold. By selecting a common air pressure and appropriate water pressures, droplet distributions can be created which, when combined, have a distribution which approximates the freezing drizzle, MVD < 40 μm condition. The approach is described more fully in Ref. 3. Figure 2 shows the two individual distributions as well as the combined distribution.

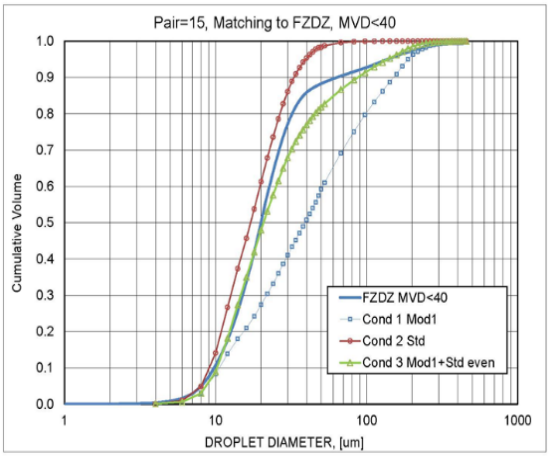

Figure 2. Normalized cumulative volume plot for data corresponding to Mod1, Standard, and combined nozzle sprays plotted alongside the Appendix O, FZDZ, MVD< 40μm distribution.

B. Model Description

The model used in this effort was a 21-inch chord, NACA 0012 airfoil model. The model is shown mounted in the test section of the IRT in Figure 3. The model is made of aluminum and has a removable leading edge. The model is equipped with 49 pressure taps and two thermocouples were mounted to the surface. The model was mounted vertically in the tunnel on the turntable located at the center of the test section.

Figure 3. 21-inch chord, NACA 0012 airfoil model mounted vertically in the test section of the IRT.

The pressure taps were used to determine the zero-degree angle of attack position by checking that the pressure profiles on both surfaces of the airfoil overlapped. The thermocouple was used to evaluate when the model had come into equilibrium with the surrounding airflow. The removable leading edge capability was not used for this effort.

C. Experimental Approach

For this work, the objective was to record and examine the ice shapes that were produced by the bimodal droplet distribution and compare that to the ice shapes produced from a similar droplet distribution that was not bimodal in nature. This was accomplished by utilizing the droplet distribution shown in Figure 2 for one set of conditions and selecting a standard single nozzle distribution, hereinafter called the standard distribution, which had a profile close to that of the bimodal distribution. The standard distribution selected is shown in Figure 4. The liquid water content values for each distribution are significantly different. The bimodal distribution has a minimum LWC of 1.45 g/m^3 at an air speed of 250 knots while the standard distribution has a minimum LWC of 0.37 g/m^3 at the same air speed. Thus, in order to compare ice shapes of the bimodal and standard distributions, scaling was required. For this research, the Olsen method[4] was used in order to maintain the same model leading edge accumulation size and freezing fraction for both sets of spray distributions over the range of icing conditions tested.

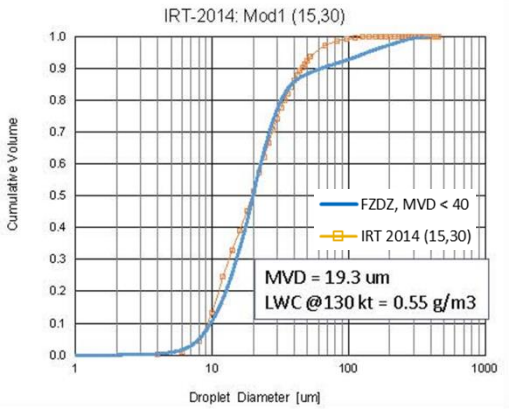

Figure 4. Comparison of the IRT Mod1 nozzle spray to the Appendix O, FZDZ, MVD < 40μm distribution at an airspeed of 130 knots.

Each test run was conducted in the following manner. The tunnel temperature and velocity conditions were set. The spray bar air and water pressures were set. The tunnel was run at the set temperature and velocity conditions and the thermocouples on the model were monitored. When the model temperature matched the tunnel static air temperature, the model was considered to be sufficiently cold to initiate the spray. The spray was initiated and lasted for the prescribed time for the icing condition of that run.

After the spray was stopped and the tunnel velocity was reduced to idle conditions, personnel entered the test section and performed the following tasks. Photographs of the ice on the model were taken from several pre-set locations around the model. A laser scanner system was used to obtain geometric data of the ice shape using the method described by Lee, et al.[5]. Once the ice shapes were scanned, a 12 inch spanwise section of the ice shape was removed from the surface into a collection tray and weighed in order to obtain the accumulated mass. Following the removal of the mass, the model surface was cleaned of all remaining ice and prepared for the next test run.

Examples of the photographs and scans from the testing are shown in Figures 5 and 6, respectively. These results are from test AE2741 which will be described below. The photograph and scan are not at the same angle or from the same exact spot along the span and are thus only representative of the data for that run.

Figure 5. Photograph of leading edge ice accretion on a 21-inch chord NACA 0012 airfoil. Test number AE2741.

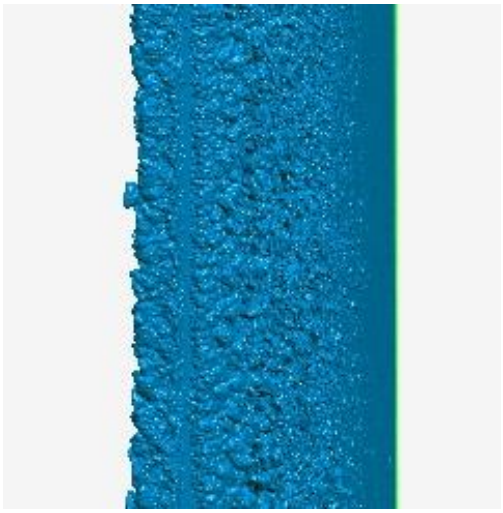

Figure 6. Scan of leading edge ice accretion on a 21-inch chord NACA 0012 airfoil. Test number AE2741.

D. Test Conditions

The test conditions chosen were based upon what could be produced using the bimodal droplet condition that has been developed for use in the IRT and on previously tested conditions using this model. The previously tested conditions shall be referred to as reference conditions. The reference conditions from previous test programs are shown in Table 1.

Test Conditions									
Case	Reference Condition	α^0	V (kts)	MVD (mm)	LWC (g/m^3)	T_t (^oC)	T_s (^oC)	Time (min)	n_0
Ice Shape Repeatibility Run 3	1	4	200	20	0.55	-5.6	-10.8	7	0.52
Ice Shape Repeatibility Run 23	2	4	130	22	1	-5.6	-7.8	6	0.34
5-15-06/Run 14	3	0	150	30	1.34	-12.5	-15.5	5.5	0.49
5-15-06/Run 15	4	0	100	30	1.75	-13.5	-14.8	6.7	0.5
3-28-05/Run 6	5	0	250	26.8	0.56	-5.2	-13.4	8.5	0.46

Table 1. Reference conditions used to scale current test conditions and to evaluate the scaling capability.

These reference cases were then used to scale both the standard and bimodal distribution cases to be tested in this effort. There were five reference cases chosen. However, due to time constraints, only four sets of standard and bimodal cases were actually run, those corresponding to reference case run numbers 1, 2, 3 and 5 from Table 1. The actual test conditions run during this research are shown in Table 2. From this table, the run numbers are shown next to the associated reference case and the runs marked with the letter a are the bimodal distribution version of that condition while those marked with the letter b are the standard distribution versions of the reference condition.

Test Conditions													
Run #	Reference Condition	α^0	V (kts)	MVD (mm)	LWC (g/m^3)	T_t (°C)	T_s (°C)	Time (min)	n_0	*Mod-1* p_{air}, psig	*Mod-1* Dp, psid	*Std* p_{air}, psig	*Std* Dp, psid
AE2716	5.b	0	250	19.3	0.37	-2.3	-10.5	14	0.46	15	30		
AE2717	2.b	4	130	19.3	0.55	-2.8	-5	11.5	0.34	15	30		
AE2718	1.b	4	200	19.3	0.42	-3.9	-9.2	9.3	0.52	15	30		
AE2719	2.a	4	130	20.8	2.15	-9.9	-12.1	2.9	0.34	15	80	15	7
AE2720	5.a	0	250	20.8	1.45	-11.9	-20.2	3.5	0.46	15	80	15	7
AE2721	1.a	4	200	20.8	1.64	-15.2	-20.5	2.3	0.52	15	80	15	7
AE2738	5.b	0	250	19.3	0.37	-2.3	-10.5	14	0.46	15	30		
AE2739	2.b	4	130	19.3	0.55	-2.8	-5	11.5	0.34	15	30		
AE2740	3.b	0	150	19.3	0.5	-4.2	-7.2	17	0.49	15	30		
AE2741	2.a	4	130	20.8	2.15	-9.9	-12.1	2.9	0.34	15	80	15	7
AE2742	3.a	0	150	20.8	1.96	-14.9	-17.9	4.2	0.49	15	80	15	7

Table 2. Standard and bimodal test conditions based upon scaling of reference conditions.

Examination of the tables shows that the freezing fraction, n_0, of the tested conditions match those of the reference conditions. The duration of each spray was altered to match the accumulation parameter as prescribed by the Olsen method and the velocity values were matched from reference conditions to actual tested conditions.

III. Results and Discussion

A. Comparison of bimodal and standard droplet distribution ice shape characteristics

The results of the comparison of each case to the corresponding reference cases will be discussed. Cross-sectional cuts in the scanned data corresponding to the location at the center of the span of the airfoil are shown in Figures 7 through 14. In these plots, the abbreviation CL stands for the Center Line cut. Each figure displays the cross-sectional cut compared to the reference tracing upon which the test condition was scaled. Table 3 provides a summary of the measured mass and volume data for each run along with mass and volume differences between the standard and bimodal distributions as well as the effective density value, ρ_{eff}, which will be described below.

Test Results											
Reference Condition	Mass bimodal (g)	Mass standard (g)	Δm_i (g)	Δm_i %	Volume bimodal in^3	Volume standard in^3	ΔVol. in^3	ΔVol. %	$\rho_{eff,b}$ g/in^3	$\rho_{eff,s}$ g/in^3	$\Delta\rho_{eff}$ %
1	163.1	131.2	31.9	24%	13.67	12.39	1.28	10.3%	11.9	10.6	12.7%
2	151.9	137.9	14	10%	14.3	11.28	3.02	26.8%	10.6	12.2	-13.1%
3	207.1	188	19.1	10%	18.46	15.49	2.97	19.2%	11.2	12.1	-7.6%
5	228.5	157.8	70.7	45%	19.52	13.56	5.96	44.0%	11.7	11.6	0.6%

Table 3. Mass and volume measurements for the ice shapes resulting from the scaled standard and bimodal distribution icing conditions from this test program.

Figures 7 and 8 show the comparison of the standard distribution and bimodal distribution results, respectively, compared to the reference condition 1. Figure 7 is an indication of the capability of the Olsen scaling method since both ice shapes are the result of unimodal droplet size distributions. In this case, although there are differences in the details of the profile, the major characteristics such as stagnation point ice thickness, upper and lower surface horn heights, and impingement limits are matched quite well. Figure

8 shows that the bimodal distribution has an impact on characteristics like the horn height and the impingement limits. The results also indicate that the stagnation point ice thickness matches quite well.

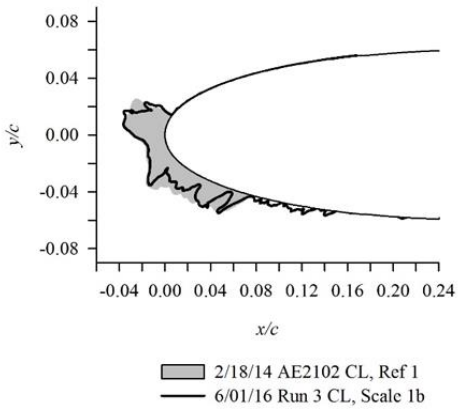

(c) n_0 = 0.52; V = 200 kt;
MVD = 19.3 μm, LWC = 0.42 g/m^3 (1b, Mod1 (15,30));
MVD = 20.0 μm, LWC = 0.55 g/m^3 (Ref 1, Mod1 (21.7, 60))

Figure 7. Mid-span profiles of leading edge ice accretion on a 21-inch chord NACA 0012 airfoil. Reference condition 1 and test number AE2718.

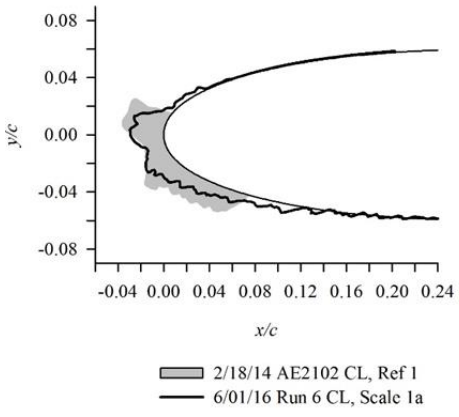

(c) n_0 = 0.52; V = 200 kt;
MVD = 20.8 μm, LWC = 1.64 g/m^3 (1a, Bimodal (15,80), (15,7))
MVD = 20.0 μm, LWC = 0.55 g/m^3 (Ref 1, Mod1 (21.7, 60))

Figure 8. Mid-span profiles of leading edge ice accretion on a 21-inch chord NACA 0012 airfoil. Reference condition 1 and test number AE2721.

There were no mass measurements made for the reference cases. The results from runs 1a and 1b had mass values of 163.1 grams and 131.2 grams, respectively. This means a net mass difference of 31.9 grams or a 24% increase in mass collected for nominally the same icing condition when the droplet distribution is bimodal rather than a standard distribution.

The volume of ice was also determined via use of the scanned ice shape data and the capability of the Geomagic Wrap[6] commercial software package to determine the volume of a closed, water-tight geometry. For the ice shapes discussed in this document, the volume was the same 12-inch spanwise section corresponding to the ice shape removed from the model for mass measurement. The results from runs 1a and 1b had ice shape volume values of 13.67 in^3 and 12.39 in^3, respectively. This means a net volume difference of 1.28 in^3 or a 10.3% increase in ice shape volume for the bimodal ice shape over the standard distribution ice shape.

These results translate into effective density values of 11.9 g/in^3 and 10.6 g/in^3 or a 12.7% increase for the bimodal ice accretion. The term effective density refers to the fact that this is not the physical density of the ice itself. The effective density can be affected by two major elements; the amount of air trapped in the ice accretion and the fact that the scanning method, based upon its line-of-sight process, has some difficulty in documenting small concave regions of ice embedded in all ice shapes. Assuming this latter source of uncertainty is nominally the same for similar ice shapes, this effective density can still be used to provide a means of comparison from one ice shape to another.

It's not clear why there was a 24% increase in mass while only a 10.3% increase in volume for the bimodal ice shape. It does suggest that the process of ice accretion may be a bit different as a result of the different droplet distributions and not just a difference in the amount of mass collected. This is just one data point and additional data needs to be collected to determine whether this is a persistant trend or just a manifestation of the data collection and processing efforts.

Figures 9 and 10 show the comparison of the standard distribution and bimodal distribution results, respectively, compared to the reference condition 2. Figure 9 is an indication of the capability of the Olsen scaling method since both ice shapes are the result of unimodal droplet size distributions. The current ice shape agrees pretty well in overall shape with the reference condition, although the overall shape seems a bit smaller than the reference condition it seems to be within repeatability norms. Figure 10 shows that the bimodal distribution has an impact on characteristics like the horn height and the impingement limits. The results also indicate that the stagnation point ice thickness matches quite well.

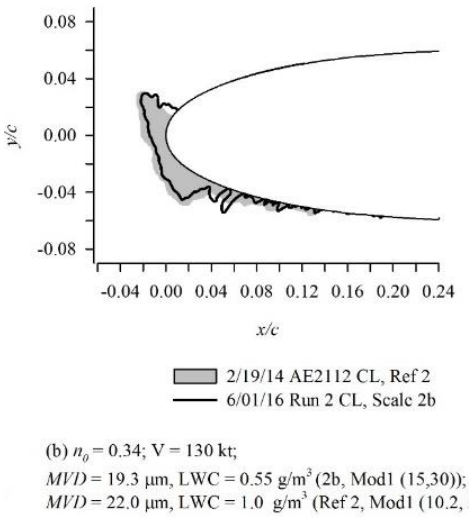

Figure 9. Mid-span profiles of leading edge ice accretion on a 21-inch chord NACA 0012 airfoil. Reference condition 2 and test number AE2717.

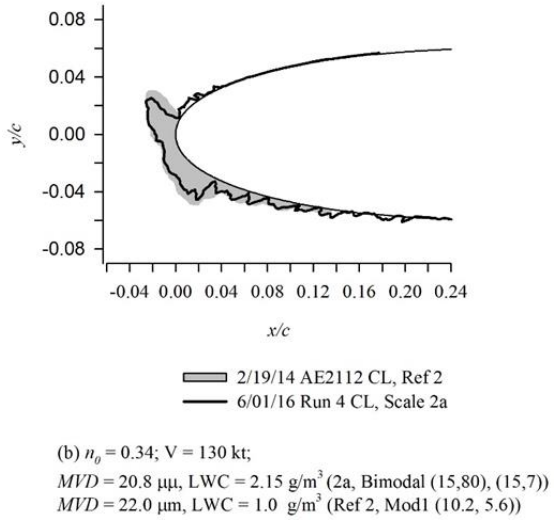

Figure 10. Mid-span profiles of leading edge ice accretion on a 21-inch chord NACA 0012 airfoil. Reference condition 2 and test number AE2719.

The results from runs 2a and 2b had mass values of 151.9 grams and 137.9 grams, respectively. This means a net mass difference of 14.0 grams or a 10% increase in mass collected for nominally the same icing condition when the droplet distribution is bimodal rather than a standard distribution. The results from runs 2a and 2b had ice shape volume values of 14.30 in^3 and 11.28 in^3, respectively. This means a net volume difference of 3.02 in^3 or a 26.8% increase in ice shape volume for the bimodal ice shape over the standard distribution ice shape. These results translate into effective density values of 10.6 g/in^3 and 12.2 g/in^3 or a 13.1% decrease for the bimodal ice accretion.

Figures 11 and 12 show the comparison of the standard distribution and bimodal distribution results, respectively, compared to the reference condition 3. Figure 11 is an indication of the capability of the Olsen scaling method since both ice shapes are the result of unimodal droplet size distributions. The current ice shape doesn't agree as well in overall shape with the reference condition as in the previous two cases. Figure 12 shows that the bimodal distribution actually appears to have better agreement with the reference condition than the standard distribution run. The chordwise extent of the bimodal ice shape is further back than that of the standard distribution ice shape. This appears to be closer to the icing limits of the refernce condition. The results also indicate that the stagnation point ice thickness matches well for both the standard and biomodal distributions.

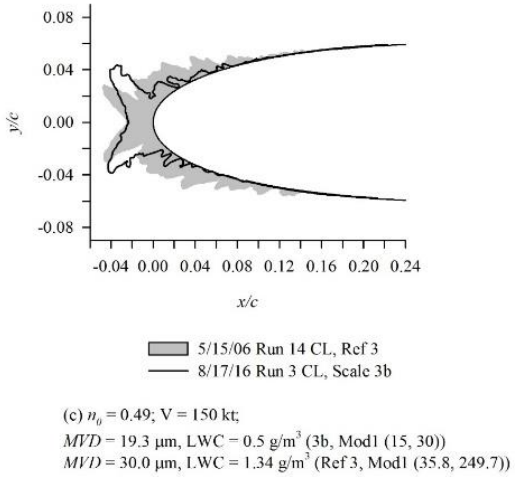

(c) n_0 = 0.49; V = 150 kt;
MVD = 19.3 μm, LWC = 0.5 g/m^3 (3b, Mod1 (15, 30))
MVD = 30.0 μm, LWC = 1.34 g/m^3 (Ref 3, Mod1 (35.8, 249.7))

Figure 11. Mid-span profiles of leading edge ice accretion on a 21-inch chord NACA 0012 airfoil. Reference condition 3 and test number AE2740.

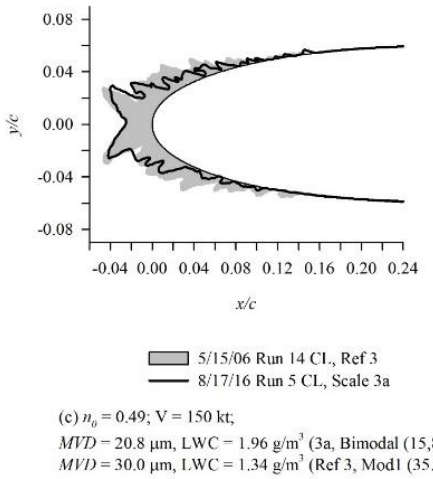

(c) n_0 = 0.49; V = 150 kt;
MVD = 20.8 μm, LWC = 1.96 g/m^3 (3a, Bimodal (15,80), (15,7))
MVD = 30.0 μm, LWC = 1.34 g/m^3 (Ref 3, Mod1 (35.8, 249.7))

Figure 12. Mid-span profiles of leading edge ice accretion on a 21-inch chord NACA 0012 airfoil. Reference condition 3 and test number AE2742.

The results from runs 3a and 3b had mass values of 207.1 grams and 188.0 grams, respectively. This means a net mass difference of 19.1 grams or a 10% increase in mass collected for nominally the same icing condition when the droplet distribution is bimodal rather than a standard distribution. The results from runs 3a and 3b had ice shape volume values of 18.46 in^3 and 15.49 in^3, respectively. This means a net volume difference of 2.97 in^3 or a 19.2% increase in ice shape volume for the bimodal ice shape over the standard distribution ice shape. These results translate into effective density values of 11.2 g/in^3 and 12.1 g/in^3 or a 7.6% decrease for the bimodal ice accretion.

Figures 13 and 14 show the comparison of the standard distribution and bimodal distribution results, respectively, compared to the reference condition 5. Figure 13 is an indication of the capability of the Olsen scaling method since both ice shapes are the result of unimodal droplet size distributions. As in the previous

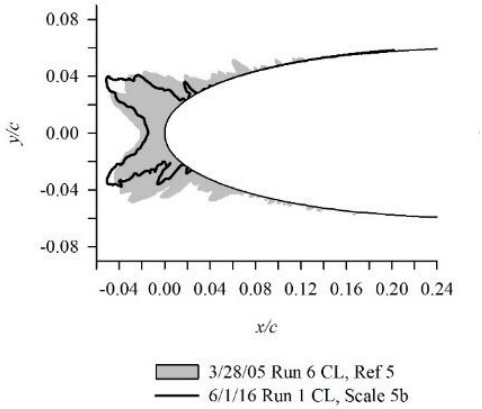

(a) n_0 = 0.46; V = 250 kt;
MVD = 19.3 μm, LWC = 0.37 g/m^3 (5b, Mod1 (15,30));
MVD = 26.8 μm, LWC = 0.56 g/m^3(Ref 5, Mod1 (16.3, 64.2))

Figure 13. Mid-span profiles of leading edge ice accretion on a 21-inch chord NACA 0012 airfoil. Reference condition 5 and test number AE2716.

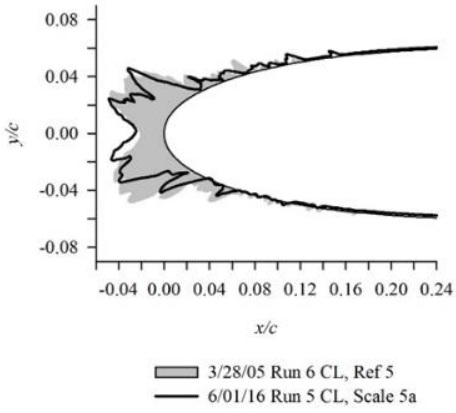

(a) n_0 = 0.46; V = 250 kt;
MVD = 20.8 μm, LWC = 1.45 g/m^3 (5a, Bimodal, (15,80), (15,7))
MVD = 26.8 μm, LWC = 0.56 g/m^3(Ref 5, Mod1 (16.3, 64.2))

Figure 14. Mid-span profiles of leading edge ice accretion on a 21-inch chord NACA 0012 airfoil. Reference condition 5 and test number AE2720.

comparison, the current ice shape doesn't agree as well in overall shape with the reference condition as in the first two cases. Figure 14 shows that the bimodal distribution actually appears to have better agreement with the reference condition than the standard distribution run. The chordwise extent of the bimodal ice shape is further back than that of the standard distribution ice shape. This appears to be closer to the icing limits of the reference condition. The results also indicate that the stagnation point ice thickness matches well for both the standard and biomodal distributions.

The results from runs 5a and 5b had mass values of 228.5 grams and 157.8 grams, respectively. This means a net mass difference of 70.7 grams or a 45% increase in mass collected for nominally the same icing condition when the droplet distribution is bimodal rather than a standard distribution. The results from runs 5a and 5b had ice shape volume values of 19.52 in^3 and 13.56 in^3, respectively. This means a net volume difference of 5.96 in^3 or a 44.0% increase in ice shape volume for the bimodal ice shape over the standard distribution ice shape. These results translate into effective density values of 11.7 g/in^3 and 11.6 g/in^3 or a negligible decrease for the bimodal ice accretion.

The results of these four comparisons indicate a consistent increase in the mass of ice accumulated for the bimodal distribution. The volume of ice also increased for the bimodal distributions at all icing conditions. However, there was inconsistent variation in both measurements for all icing conditions tested. This led to no particular trend to the effective density value. This is only for four conditions and more data is needed to determine if any such trend can be identified.

B. Examination of limited repeatability information for ice accretion measurements

The results described in section A provide some information regarding the variation of ice shape due to the change from a standard droplet distribution to a bimodal droplet distribution. However, to judge whether these differences are significant or not, repeat runs at the same icing condition are used to determine the natural variability of ice accretion characteristics. For the NACA 0012 model tested in this effort, we were only able to repeat one test condition. For this research effort, the repeat case was chosen to be reference condition 2. Figures 15 and 16 show the ice shapes for test conditions 2a and 2b respectively.

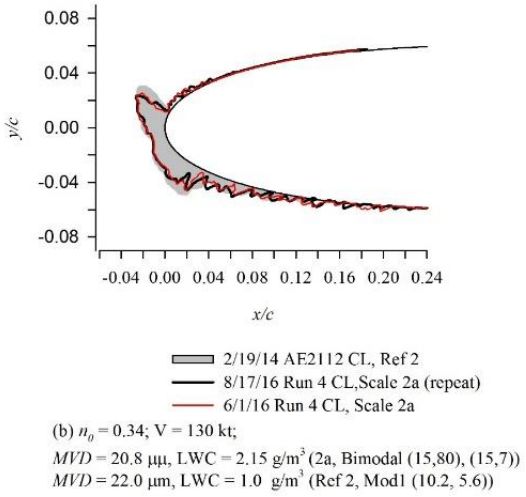

Figure 15. Mid-span profiles of leading edge ice accretion on a 21-inch chord NACA 0012 airfoil. Reference condition 2 and test numbers AE2719 and AE2741.

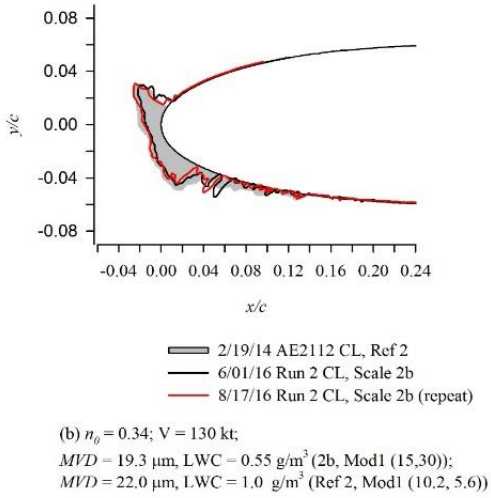

Figure 16. Mid-span profiles of leading edge ice accretion on a 21-inch chord NACA 0012 airfoil. Reference condition 2 and test numbers AE2717 and AE2739.

The results from repeat runs of 2a (AE2719 and AE2741) had mass values of 151.9 grams and 139.2 grams for the repeat run. This means a net mass difference of 12.7 grams or a 8.4% difference in mass collected for nominally the same icing condition when the droplet distribution is bimodal. The 2a repeat case results had ice shape volume values of 14.30 in^3 and 12.36 in^3 for the repeat run. This means a net volume difference of 1.94 in^3 or a 13.6% difference in ice shape volume for the bimodal ice shape. These results translate into effective density values of 10.6 g/in^3 and 11.3 g/in^3 or a 6.6% difference for the bimodal distribution ice accretion.

The results from repeat runs of 2b (AE2717 and AE2739) had mass values of 137.9 grams and 133.0 grams for the repeat run. This means a net mass difference of 4.9 grams or a 3.6% difference in mass collected for nominally the same icing condition when the droplet distribution is the standard shape. The 2b repeat case results had ice shape volume values of 11.28 in^3 and 10.61 in^3 for the repeat run. This means a net volume difference of 0.67 in^3 or a 5.9% difference in ice shape volume for the standard distribution ice shape. These results translate into effective density values of 12.2 g/in^3 and 12.5 g/in^3 or a 2.4% difference for the standard distribution ice accretion.

These results suggest that the difference between the ice shapes generated with the standard distribution and the bimodal distribution are marginally larger than the repeatability of the same parameters for either distribution. The case chosen for this comparison was for the condition having the smallest variations. It is expected that there would be a greater effect apparent for the other conditions examined. More data is needed to determine any trends.

Examination of these results does suggest one trend. As the airflow velocity increases the mass differences between the standard and bimodal droplet distribution results seems to increase. Since each reference condition cloud has a different water mass flux, this trend is best illustrated by plotting the ice mass difference between the standard and bimodal ice shapes normalized by the total water mass passing through the projected upstream area of the model. This total water mass for each run can be determined from the expression shown in Eq. 1.

$$M_w = LWC \cdot V \cdot t \cdot A_p \tag{1}$$

where LWC is Liquid Water Content, V is airflow velocity, t is exposure time, and A_p is the projected area of the airfoil. The projected area is the thickness of the model times the span length used for collection of the ice mass. The span length used in all the runs for this test program was 12 inches. The thickness of the airfoil is dependent upon the angle of attack and was therefore 12% chord for the 0.0 deg conditions and 13.1% chord for the 4.0 deg conditions.

The normalized ice mass difference is the difference in measured ice mass between the standard case and the bimodal case divided by the average total water mass value for the two cases. This relationship is determined from the expression shown in Eq. 2.

$$\Delta\widetilde{m}_i = \Delta m_i / \overline{M_w} \tag{2}$$

This is shown in Figure 17. Although there is little change in $\Delta\widetilde{m}_i$ from 130 knots to 150 knots, the general trend is for the mass difference to increase as the velocity increases. The slight decrease from 130 knots to 150 knots could certainly be attributed to experimental variability. A larger sample of results is needed to further evaluate this trend. The results of these tests also show that the chordwise extent of the ice shape is always further aft for the bimodal distribution than for the standard distribution. This suggests that the approximately ten percent of the bimodal cloud which is at droplet diameters above 100 μm, and which is not present in the standard distribution, may be having a greater influence on the final ice

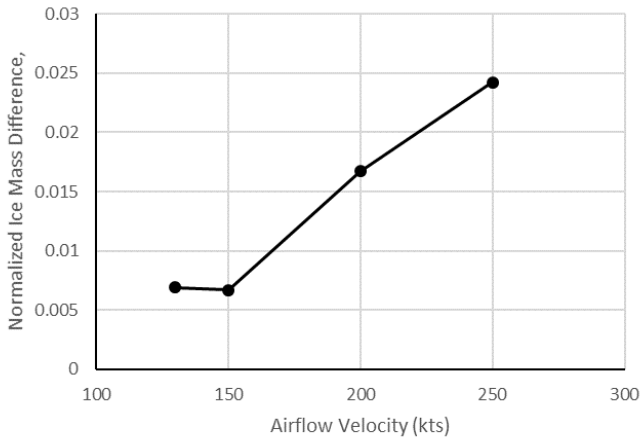

Figure 17. Difference in accumulated ice mass from bimodal and standard distributions for equivalently scaled conditions as a function of airspeed in the tunnel.

deposition as the velocity increases. As in the other results, this is a trend that should be evaluated further through examination of additional data.

IV. Conclusion

An initial dataset of ice shapes accreted under bimodal droplet distribution conditions in the NASA Icing Research Tunnel has been produced. The ice shapes from the bimodal clouds were compared to equivalent ice shapes from a standard droplet distribution cloud where pertinent characteristics such as accumulation parameter and freezing fraction were the same based upon use of the Olsen scaling method. Ice shape photographs, laser scans of the ice, and measurements of the ice mass were obtained to enable comparison of the bimodal and standard distribution ice accretions.

Initial results indicate that there were differences in the mass and volume of ice between the two distributions. These differences were compared to repeatability measurements for a given icing condition and found to be slightly more than the repeatability measurements. Since the number of conditions measured are limited it is difficult to discern any such trends. More data is needed to determine whether there is a significant difference in ice mass or ice volume as a result of droplet distribution differences.

There did appear to be a trend in the mass difference between bimodal and standard distributions as a function of airspeed. There also was a noticeable increase in the chordwise extent of the ice accumulation for the bimodal distribution. This could be due to the approximately ten percent of cumulative volume contained in droplet sizes larger than 100 μm present in the bimodal distribution that is not found in the standard distribution.

Although more data is needed to discern trends, this effort provided some insight into the characteristics that differentiate single spray conditions from bimodal spray conditions. At this time, it has not been determined whether bimodal spray cloud recreation is necessary for accurate reproduction of SLD icing conditions.

References

[1] Steen, L.E., Ide, R.F., Van Zante, J.F., and Acosta, W. J., "NASA Glenn Icing Research Tunnel: 2014 and 2015 Cloud Calibration Procedure and Results," NASA/TM—2015-218758, May 2015.

[2] CFR 14, Part 25, Appendix O, "Supercooled Large Drop Icing Conditions," http://www.ecfr.gov.

[3] King-Steen, L. E. and Ide, R. F., "Creating a Bimodal Drop-Size Distribution in the NASA Glenn Icing Research Tunnel," AIAA Paper 2017-XXXX, June 2017.

[4] Anderson, David N., "Manual of Scaling Methods," NASA/CR—2004-212875, March 2004.

[5] Lee, S., Broeren, A.P., Kreeger, R.E., Potapczuk, M., and Utt, L., "Implementation and Validation of 3-D Ice Accretion Measurement Methodology," AIAA 6th Atmospheric and Space Environments Conference, Atlanta, GA, June 16-20, 2014, AIAA Paper 2014-2613.

[6] Geomagic Wrap, http://www.geomagic.com/en/products/wrap/overview, 3D Systems Corp., April 27, 2017.